Middle-East Journal of Scientific Research 22 (6): 809-815, 2014
ISSN 1990-9233

DOI: 10.5829/idosi.mejsr.2014.22.06.21951

A Novel Faulty Diagnosis Technique of Three-Phase Induction Motor Based on Wavelet Packets and SOM-SVM

S. Jaya and R.Vinodha

Department of Electronics and Instrumentation Engineering,
Annamalai University, Chidambaram Tamilnadu, India

Abstract: Due to their advantages over other electrical motors, highly reliable three phase induction motor plays crucial role in the industrial applications. Most of the researchers have considered motor-diagnosis techniques to prevent sudden stops by the main sources of faults; 1.Bearingfaults 2.Statorfaults 3. Rotor Faults 4. Eccentricity Faults. The lack of an accurate coherent model is the main difficult to describe a faulty motor. The objective of this paper proposed a Self Organizing Map-Support Vector Machine (SOM-SVM) to accurate classification. From the faults of the induction motor and the sensor signal information, Wavelet Packet Transformation (WPT) is utilized to detect and extract the fault feature vectors from stationary or non-stationary signals. Then SOM-SVM classifies the pattern information. The results show that the detection of the fault, identification of the fault is improved and more accurately classified.

Key words: Empirical Mode Decomposition (EMD) · Intrinsic Mode Functions (IMF) · Wavelet Packet Transformation (WPT) · Self Organizing Map-Support Vector Machine (SOM-SVM).

INTRODUCTION

Induction motor [1-2] plays a vital part in the industrial applications in an extensive range of operating regions because of its more reliable, simple, healthy structure and less manufacture costs. However, the machine finally gets faulteddueto heavy duty cycles, failed during installation and manufacturing factors etc. Bearing Faults [3] contain above 40% from all kinds of machine failures. Bearings are regular components of all electrical machines. Essentially bearings comprise of two concentric rings which are categorized as the local and the distributed rings. A set of balls positioned in raceways rotate inside these rings. A consistent stress on the bearing results in the exhaustion failures. This kind of failure results in discernible vibrations and increased noise levels. Contamination, improper lubrication and brinelling are liable for the bearing fault. Mostly the stator faults [4] occur almost 30%-40% in induction motors because of insulation breakdown. This is most important to detect faults in time since fault can prompt to the whole destruction of the induction motor. Rotor faults occurs 10% faults of whole induction motor failures because of the rotor winding. Rotor faults [5] of the induction motors have mostly broken rotor bars as a result of torque pulsation, overheating and arcing.

Eccentricity [6] related faults exists an unequal air gap between stator and rotor. And 10% of an air gap eccentricity is allowable. When this fault gets to be bigger, the unbalanced radial forces can prompt stator and rotor rub and then stator and rotor core can get damaged. Static and Dynamic eccentricities are two parts of eccentricity.

The stator or rotor core is wrong positioning at the starting stage results into static eccentricity. In the dynamic eccentricity, the rotor position is not at the center of the rotation. The minimum air gap position rotates with the rotor. This misplacement is caused by the bent rotor shaft and bearing wear. The oscillations of mechanical components of the motors are common processes in induction motors, called as Vibrations. These oscillations are reflected in the machine shaft. If the faults are not predicted, it may pose unreliability and unsafe operation.

Corresponding Author: S. Jaya, Department of Electronics and Instrumentation Engineering,
Annamalai University, Chidambaram Tamilnadu, India.

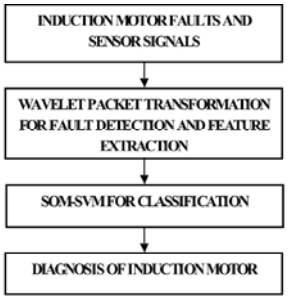

Fig. 1: Block diagram of the new fault diagnostic method

However, numerous methods have been proposed for fault detection and diagnosis, but most of the methods have been succeeded. Generally, sensors are utilized to collect time domain current signals in the motor fault diagnosis process. In the diagnosis process, both time and frequency domain signals have been utilized to analyze the motor condition and find out the existed faults in the motor. Many researchers have proposed different types of diagnostic techniques in the past years. To diagnose the fault automatically in the induction motors, many proposed soft computing techniques enhance the precision and accuracy. In recent years, without detailed analysis of fault and without system modeling required, electrical machines have moved from conventional techniques to computerized techniques, such as genetic algorithms, neural networks and fuzzy logics. These techniques need at least intelligence configuration. Fast Fourier Transform (FFT) [8-9] performs adequately for stationary signals. For non-stationary signals, FFT is not suitable to evaluate the signal. However, the time duration of each fault is obtained as characteristics of the system. As per the above standards, a new fault diagnosis technique is proposed in this paper. Figure 1 depicts that the multiple faults has been occurred in the induction motor[10].

Hence, the sensor signal plays an essential role for the diagnosing of faults to select a suitable signal by observing vibration, noise and torques. Due to the costly sensors, the motor current is utilized for diagnosis of faults. Hence, motor current can be successfully distinguished healthy as well as faulty motor waveforms[11]. Based on stationary or non-stationary signals, WPT [12] is utilized to detect and extract the fault feature vectors. To classify the extracted vectors, first, a Self Organizing Map(SOM) network is processed in an unsupervised way with the unlabeled patterns.

Then by using corresponding neural weight vectors, find the average distance of a neuron and its neighbor neuron in the output layer. Hence, the input space neuron mapping samples of the low-density regions have better average neighbor distance than the high-density regions. The classified technique SVM would be processed with the available labeled samples. After processing, find the accurate classification of each unlabeled sample with the assist of the processed SVM. Then, the h_1 unlabeled samples have selected with the lowest classification confidence and mapped into distinct neurons of the SOM. The main advantage is that when biased initial training samples are examined, then the higher precision training samples place very close to the decision boundary between classes.

This paper can be organized as follows. Section II describes the wavelet packet Transformation to detect and extract the fault, section III describes the SOM-SVM for classification, section IV discussed the result and section V summarizes the conclusion of this paper.

Wavelet Packet Transformation: The WPT technique is a generalization of Wavelet Transform (WT) decomposition. It states that a signal can be transformed from time domain to frequency domain in each level. In first level wavelet decomposition, a signal can be split into an approximation coefficient and a detail coefficient, shown in Figure 2. In second level decomposition, the approximation coefficient is again split into approximation and detail coefficients and then repeats the level of process.

In Wavelet Packet Transformation (WPT), both the approximations and the details can be split, shown in Figure.3. In WPT generalization, the low pass (approximation) and highpass (detail) coefficient elements output can be iterated into more filtering. Hence the WPT does more than one wavelet packet at a given scale at the iteration of high pass filter. But the low pass filter is repeated at each level in wavelet transform. The final level of the wavelet packet decomposition is the time representation of the signal. At each level, the tradeoff between time resolution and frequency resolutions can be increased. Hence, the WPT obtains aprecise frequency resolution than the WT. For a given sequence of signals $x_{jn} \in l_2$at scale j, the approximation coefficients can be derived by filtering x_{jn} with the low-pass wavelet filter $H = \{h_t\}$ andthen sub sampled by two

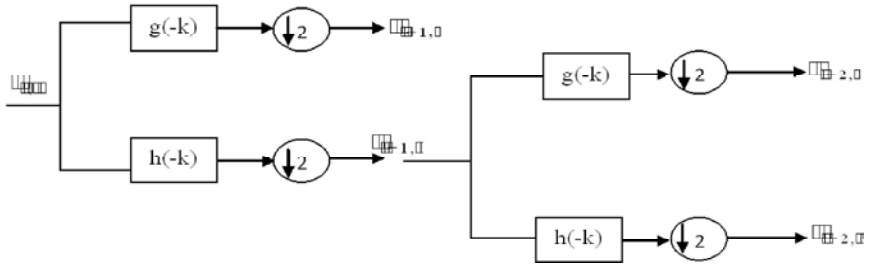

Fig. 2: Decompositions of Wavelet Transform

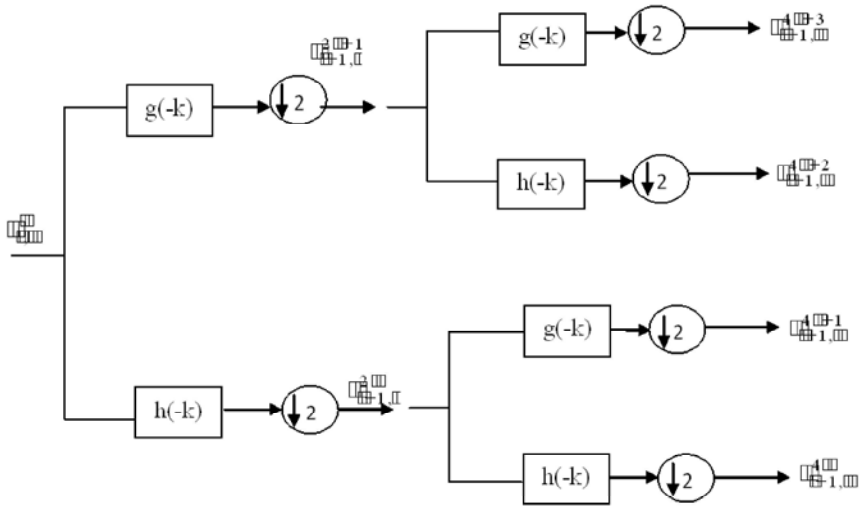

Fig. 3. Decompositions of Wavelet Packet Transformation

$$x_{j+1,k} = \sum_n h_{n-2k}\, x_{j,n} \tag{1}$$

Few details would have been lost from x_{jn} because of low-pass filtering, which could be computed by filtering x_{jn} with the high-pass wavelet filter $G = \{g_t\}$ and then sub sampled by two

$$d_{j+1,k} = \sum_n d_{n-2k}\, x_{j,n} \tag{2}$$

Here $j + 1,k$ is the detail coefficient. Hence, both equations (1) and (2) are considered as a decomposition signal onto an orthogonal and the reconstruction can be considered as summed up the orthogonal projections.

$$x_{j,n} = \sum_n h_{n-2k}\, x_{j+1,k} + \sum_n d_{n-2k}\, d_{j+1,k} \tag{3}$$

Here, filters h_t and g_t are assumed to satisfy

$$g_t = (-1)^t h_{1-t}, \sum_n h_t = \sqrt{2}, \sum_n h_t h_{t+2\varepsilon} = \delta_{0,\varepsilon},$$

$$\delta_{0,\varepsilon} = \begin{cases} 1, \varepsilon = 0 \\ 1, \varepsilon \neq 0 \end{cases}$$

Here t ◎ Z, ε ◎ Z.

In wavelet transform, each level can bedecomposedby passing the previous approximation coefficients ashigh filters and lowpass filters. However, in wavelet packet decomposition, both the detail coefficients (High Frequency) and approximation (Low Frequency) coefficients have been decomposed. The equations of wavelet packet coefficients can be defined as

$$x_{j+1,k}^{2l} = \sum_n h_{n-2k}\, x_{j,n}^{l} \tag{4}$$

$$x_{j+1,k}^{2l+1} = \sum_n g_{n-2k}\, x_{j,n}^{l} \tag{5}$$

The reconstructions can bedone as

$$x_{j,n}^{l} = \sum_n h_{n-2k}\, x_{j+1,k}^{2l} + \sum_n g_{n-2k}\, x_{j+1,k}^{2l+1} \tag{6}$$

Here, l is the space serial number in scale j. For l scale decomposition, the wavelet packet decomposition produces 2l sets ofcoefficients rather than j + 1 sets of coefficients for the wavelet transform. However, due to the down sampling process the number of coefficients is still same and there is no redundancy.

Denote k_j is the sequential time index at scale j, $j = 0,1,\ldots,J$. Consider the followingdata

$$X^l(k_j) \triangleq \left[x_{j,k_j}^{l\tau}, x_{j,k_j+1}^{l\tau}, \ldots, x_{j,k_j+2^{J-j}-1}^{l\tau}\right]^T \quad (7)$$

Where $x_{j,k_j}^{l\tau}$ represents the transpose of x_{j,k_j}^{l}. Theequations (4) and (5) can be derived as

$$\begin{cases} X^l(k_{j+1}) = H_j X^l(k_j) \\ X^{2l+1}(k_{j+1}) = G_j X^l(k_j) \end{cases} \quad (8)$$

Operators H_j and G_j are composed as low-pass and high-pass filter response mapping from scale j to j + 1. When mapping from scale j + 1 to j, the equation (6) can also be written as

$$X^l(k_j) = H_j^T X^{2l}(k_{j+1}) + G_j^T X^{2l+1}(k_{j+1}) \quad (9)$$

The constraint can be expressed as

$$H_j^T H_j + G_j^T G_j = I$$

And

$$\begin{bmatrix} H_j H_j^T & H_j G_j^T \\ G_j H_j^T & G_j G_j^T \end{bmatrix} = \begin{bmatrix} I & 0 \\ 0 & I \end{bmatrix}$$

To decompose $X(K_j)$ into the high frequency coefficients j, the followingdecomposition transform can be written as

$$\begin{bmatrix} X^{2^{J-j_1}}(k_j) \\ X^{2^{J-j_1+1}}(k_j) \\ \vdots \\ X^{2^{J-j_1+2^{J-j_1}-1}}(k_j) \end{bmatrix} = T^{J|j} X^l(k_j)$$

Here $T^{J|j}$ is an orthogonal matrix. It can be written as

$$T^{J|j} = \begin{bmatrix} H_{J-1}H_{J-2}\ldots H_j \\ G_{J-1}H_{J-2}\ldots H_j \\ \vdots \\ G_{J-1}G_{J-2}\ldots G_j \end{bmatrix}$$

For simplicity and efficiency, a node $x_{j+1,k_{j+1}}^{2l}$ or $x_{j+1,k_{j+1}}^{2l+1}$ can be written as the linear combination of the nodes at scale j. From the equations (4) and (5), it can be defined as

$$x_{j+1,k_{j+1}}^{2l} = \frac{\sqrt{2}}{2}\left(x_{j,k_j}^{l} + x_{j,k_{j+1}}^{l}\right)$$

$$x_{j+1,k_{j+1}}^{2l+1} = \frac{\sqrt{2}}{2}\left(x_{j,k_j}^{l} - x_{j,k_{j+1}}^{l}\right)$$

Here, t = 0, 1,H = $\{h_0, h_1\}$, G = $\{g_0, g_1\}$, $h_0 = \frac{\sqrt{2}}{2}, h_1 = \frac{\sqrt{2}}{2}, g_0 = \frac{\sqrt{2}}{2}, g_1 = -\frac{\sqrt{2}}{2}$,it can be seen that $k_j = \left[\frac{k_0}{2^j}\right]$,

Self Organizing Map-Support Vector Machine (SOM-SVM): The proposed method comprises of two steps. At first, a SOM neural network is trained in an unsupervised way inorder to recognize the available vital samples that have placed withlow-density regions of the feature space. It is achieved by updating the weight vector related to each neuron. When the network attains convergence, the weight vectors depict a mapping from the high dimensional input space to a low dimensional output space. At the training phase convergence, finds the average distance of each neuron and its neighboring neurons by utilizing their consequent weight vectors. The average distance of neighbor neuron k, indicated as $\bar{w}_k$(equation (10))

$$\bar{w}_k = \frac{1}{|N_k^r|}\sum_{i \in N_k^r} \|w_k - w_i\|^2 \quad (10)$$

Where N_k^r represent the set of neurons in the r^{th} order neighbor of the neuron k. The SOM conserves the topological property of input space. Then utilize the set of acquired average neighbor distance measures to distinguish samples be inlowdensity regions of the feature space. These distinguished samples are connected with the neurons have better average distance values. Therefore, those neurons have a higher probability of boundary samples than the lower average distance of neighbor neurons. Then, train with the accessible labeled samples n SVM binary classifiers (each one connected with different class) organized in a One-Against-All (OAA) architecture, which includes a corresponding architecture made up of n binary SVMs. Each SVM explains a two-class problem characterized by one

information class against all the others. The smallest distance between the n decision hyper planes of binary SVM classifiers with OAAis considered to compute for each unlabeled sample x in the unlabeled poolU, i.e. $x \epsilon U$ stated in equation (11)

$$s(x) = \min_{i=1,2,\ldots,n} \{|f_i(x)|\} \quad (11)$$

Based on the Multi Class Label Uncertainty (MCLU) technique, the difference among first and second largest distance values of thehyperplanes is contemplated to find the confidence value $s(x)$ of all unlabeled samples x ◎ U as stated in equation (12)

$$s(x) = f_{r_1}(x) - f_{r_2}(x) \quad (12)$$

Where

$$r_1 = \arg\max_{i=1,2,\ldots,n} \{|f_i(x)|\}$$

and

$$r_2 = \arg\max_{i=1,2,\ldots,n; i \neq r_1} \{|f_i(x)|\}.$$

Hence, the uncertainty of each unlabeled sample $(x \in U)$ is measured based on its corresponding s(x) value. Due to the lowest correct classification, the samples of lower confidence values are contemplated as the most uncertain. According to the Equations (11) and (12), h_1 samples from U have the lowest confidence valuesand mapped into different neurons of the SOM. i.e. the h_1 mostuncertain samples are varied from each other while similar input patterns are mapped into the same neuron. At that point, abatch of $h(1 < h < h_1)$ samples from the chosen h_1 samplesare selected that relate to the SOM mapping neurons highest average distances in neighbor neurons in equation (10). Then decidelabels to the selected h samples and comprisethem into the training set.

Algorithm

- By utilizing labeled and unlabeled patterns, train the SOM neural network.
- Find the average neighbor distance of each neuron utilizing equation(10)
- Repeat the steps 1 to 2.
- Train with the accessible initial labeled sample n binary SVM classifiers organized in a One-Against-All architecture.
- By utilizing either equation (11) or (12), find the $s(x)$ value of each unlabeled sample.
- Choose the h_1 samples from U which have the lowest certainty values and aremapped into different neurons of SOM.
- Choose the $h(1 < h < h_1)$ samples from the h_1 samples that correspond to the SOM mapping neurons having thehighest average neighbor distances (exploitation of the cluster assumption).
- Decide labels to the h selected samples and comprise them into the training set.
- Repeat until the condition is satisfied, the final training set is attained.

RESULT AND DISCUSSION

In this section, the proposed method discuss about the faults and fault identification and accuracy of the three phase induction motor. Table 1 is listed about the characteristics of the three phase induction motor. This motor is diagnosed for the detection of the bearing fault for vibration signal, eccentricity fault and the broken rotor bars. The induction motor condition is measured by speed and load. In this paper the speed of the induction motor subsequently measuring 200, 500, 800, 1200, 1400 rpm values with no load (0%), half load (50%) and full load (100%) values. The accuracy can be defined as

$$Accuracy = \frac{TP + TN}{TP + TN + FP + FN} = \frac{Correctly\ classified\ events}{total\ number\ of\ events}$$

Where

TP = The number of positive events correctly diagnosed as positive.
FN = The number of positive events incorrectly diagnosed as negative.
FP = The number of negative events incorrectly diagnosed as positive.
TN = The number of negative events correctly diagnosed as negative.

The accuracy of the faults can be classified by changing the speed of motor at different loads. The motor speed was diagnosed the faults of motor at 600, 800, 1000, 1200 and 1400 rpm (revolutions per minute) values with load percentages. At no load (0% load), the accuracy of the fault diagnosing is shown better results at different motor speed compared with the wavelet and Fourier transforms, shown in Table 2.

Table 1: Characteristics of an Induction Motor

Description	Value
Power	0.55 KW
Voltage	415 V
Current	1.5 A
Supply Frequency	50Hz
Number of Poles	4
Horse Power	0.75 HP
Speed	1420 rpm

Table 2: Classified Accuracy of faults at 0%load

	Accuracy of the motor speed for no load (0%)				
	Motor Speed (in Revolution per minute)				
Types of Method	600	800	1000	1200	1400
Fourier Transform	88.14%	89.49%	91.32%	93.65%	95.97%
Wavelet Transform	91.01%	92.12%	93.87%	95.98%	97.84%
PROPOSED	92.92%	94.01%	95.15%	96.28%	98.11%

Table 3: Classified Accuracy of faults at 25%load

	Accuracy of the motor speed for load (25%)				
	Motor Speed (in Revolution per minute)				
Types of Method	600	800	1000	1200	1400
Fourier Transform	87.39%	88.74%	89.98%	91.85%	93.91%
Wavelet Transform	89.47%	90.33%	91.67%	93.48%	95.14%
PROPOSED	90.55%	92.01%	93.45%	95.38%	96.25%

Table 4: Classified Accuracy of faults at 50%load

	Accuracy of the motor speed for half load (50%)				
	Motor Speed (in Revolution per minute)				
Types of Method	600	800	1000	1200	1400
Fourier Transform	81.14%	83.49%	86%	88.65%	90.67%
Wavelet Transform	83.61%	85.72%	87.07%	89.71%	92%
PROPOSED	84.32%	86.88%	89.97%	91.08%	93.51%

Table 5: Classified Accuracy of faults at 75%load

	Accuracy of the motor speed for load (75%)				
	Motor Speed (in Revolution per minute)				
Types of Method	600	800	1000	1200	1400
Fourier Transform	74.64%	77%	79.17%	81.30%	83.81%
Wavelet Transform	77.91%	80.15%	82.00%	84.47%	86.99%
PROPOSED	81.22%	83.01%	85.97%	87.78%	89.44%

Table 6: Classified Accuracy of faults at Full load (100%)

	Accuracy of the induction motor for load (100%)				
	Motor Speed (in Revolution per minute)				
Types of Method	600	800	1000	1200	1400
Fourier Transform	67.36%	70.77%	72.55%	75.57%	77.33%
Wavelet Transform	73.24%	76.54%	78.81%	81.21%	82.80%
PROPOSED	76.36%	78.05%	80.98%	83.00%	85.75%

Table 7: Classified Accuracy of faults at Maximum speed of the motor

	Accuracy of the induction motor for maximum speed 1420 rpm				
	Load %				
Types of Method	0%	25%	50%	75%	100%
Fourier Transform	96.14%	94%	92.11%	89.67%	88.20%
Wavelet Transform	98%	96.01%	93.97%	92.18%	91.10%
PROPOSED	98.32%	96.47%	95.25%	94.08%	93%

At 600, 800, 1000, 1200, 1400 rpm values of motor speed, the fault is diagnosed 92.92%, 94.01%, 95.15%, 96.28% and 98.11% of accuracy respectively. When load is increased 25%, the fault is diagnosed with the accuracy of 90.55%, 92.01%, 93.45%, 95.38% and 96.25% at 600, 800, 1000, 1200 and 1400 rpm of the motor speed respectively, shown in Table 3. In Table 4, the accuracy of the diagnosed fault at half load (50% load) are 84.32%, 86.88%, 89.97%, 91.08%, 93.51% at the motor speed of 600, 800, 1000, 1200 and 1400 rpm values respectively.

In Table 5, the load is increased to 75%, the changes of motor speed from 600, 800, 1000, 1200 and 1400 rpm values, the accuracy of diagnosed faults obtained as 81.22%, 83.01%, 85.97%, 87.78% and 89.44% respectively. And finally, at full load (100% load), 76.36%, 78.05%, 80.98%, 83.00% and 85.75% are the accuracies of the diagnosed faults at the speed of motor 600, 800, 1000, 1200 and 1400 rpm values respectively, shown in Table 6. In Table 7, the fault diagnosed accuracy are 98.32%, 96.47%, 95.25%, 94.08%, 93% for 0%,25%, 50%, 75% 100% loads respectively.

CONCLUSION

This paper proposed to diagnose the faults in the induction motor using wavelet packet transformations and SOM-SVM. Wavelet Packet Transformation (WPT) is utilized to detect the fault and then extract feature vectors from stationary or non-stationary signals. Self Organizing Map-Support Vector Machine (SOM-SVM) utilized to improve the identification of the faults and then classified more accurately. The accuracy of the diagnosed faults can be classified by variations in the motor speed at different loads. While the load increases in induction motor, vibrations of the motor grow worse. Hence, the accuracy is decreased rapidly. However, the accuracy of the proposed method is better than Wavelet and Fourier transformations.

REFERENCES

1. Rockwell automation -Application basics of operation of three-phase induction motors, 1996, pp: 1-59.
2. Edward J. Thornton and J. Kirk Armintor, 2003. The Fundamental of AC Electric Induction Motor Design and Application, proceedings of the 20th international pump user's symposium, pp: 95-106.
3. Nawal A. Hussein and DhariYousif Mahmood, 2012. 3-phase Induction Motor Bearing Fault Detection and Isolation using MCSA Technique based on neural network Algorithm, Journal of Engineering and Development, 16(3): 175-189.
4. Fatiha Zidani and Mohamed Benbouzid, 2003, Induction Motor Stator Faults Diagnosis by a Current Concordia Pattern Based Fuzzy Decision System, IEEE Transactions on Energy Conversion, 18(4): 469-475.
5. Didier G. and E. Ternisien, 2006. Fault Detection of Broken Rotor Bars in Induction Motor Using a Global Fault Index, IEEE Transactions on Industry Applications, 42(1): 79-88.
6. Bashir Mahdi Ebrahimi and Jawad Faiz, 2011. Eccentricity fault identification in round rotor synchronous motors considering load variation, Elektrotechniczny (Electrical Review), ISSN 0033-2097, pp: 289-292.
7. Watson, M. and J. Sheldon, 2007. A Comprehensive High Frequency Vibration Monitoring System For Incipient Fault Detection and Isolation Of Gears, Bearings And Shafts/Couplings In Turbine Engines And Accessories, ASME, pp: 1-10.
8. Seungdeog Choi and B. Akin, 2010. Implementation of a Fault-Diagnosis Algorithm for Induction Machines Based on Advanced Digital-Signal-Processing Techniques, IEEE Transactions on Industrial Electronics, 58(3): 937-948.
9. Pineda Sanchez, M. Antonino-Daviu and J. Roger-Folch, 2010. Diagnosis of Induction Motor Faults in the Fractional Fourier Domain, IEEE Transactions on Instrumentation and Measurement, 59(8): 2065-2075.
10. Devi, N.R. and P.V.R. Rao, 2011. Wavelet-ANN based fault diagnosis in three phase induction motor, IEEE India Conference (INDICON), pp: 1-8.
11. Vijay, P. and K. Prashant, 2013. Induction Motor Condition Monitoring Using Fuzzy Logic, Advance in Electronic and Electric Engineering, 3(6): 755-764.
12. Enyu Jiang, Peng Zan and Xiaojin Zhu, 2013. Rectal sensation function rebuilding based on optimal wavelet packet and support vector machine, IET Science, Measurement and Technology, 7(3): 139-144.
13. Azgomi, H.F. and J. Poshtan, 2013. Induction motor stator fault detection via fuzzy logic, IEEE Iranian Conference on Electrical Engineering (ICEE), pp: 1-5.
14. Aydin, I., M. Karakose and E. Akin, 2007. Artificial immune based support vector machine algorithm for fault diagnosis of induction motors, IEEE International Aegean Conference on Electrical Machines and Power Electronics, pp: 217-221.